OXFORD GENETICS

GENETICS, 2023, 223(2), iyac163
https://doi.org/10.1093/genetics/iyac163
Advance Access Publication Date: 27 October 2022
Plant Genetics and Genomics

AGO1 and HSP90 buffer different genetic variants in *Arabidopsis thaliana*

Tzitziki Lemus [1,2] Grace Alex Mason [1,3] Kerry L. Bubb [1] Cristina M. Alexandre [1] Christine Queitsch [1,*] Josh T. Cuperus [1,*]

[1]Department of Genome Sciences, University of Washington, Seattle, WA 98105, USA
[2]Present address: Department of Human Genetics, University of California Los Angeles, Los Angeles, CA 90095, USA
[3]Present address: Department of Plant Biology and Genome Center, University of California, Davis, CA 95616, USA

*Corresponding author: Department of Genome Sciences, University of Washington, William H. Foege Hall, 3720 15th Ave NE, Seattle, WA 98105, USA. Email: queitsch@uw.edu (CQ); *Corresponding author: Department of Genome Sciences, University of Washington, William H. Foege Hall, 3720 15th Ave NE, Seattle, WA 98105, USA. Email: cuperusj@uw.edu (JTC)

Abstract

Argonaute 1 (AGO1), the principal protein component of microRNA-mediated regulation, plays a key role in plant growth and development. AGO1 physically interacts with the chaperone HSP90, which buffers cryptic genetic variation in plants and animals. We sought to determine whether genetic perturbation of *AGO1* in *Arabidopsis thaliana* would also reveal cryptic genetic variation, and if so, whether *AGO1*-dependent loci overlap with those dependent on HSP90. To address these questions, we introgressed a hypomorphic mutant allele of *AGO1* into a set of mapping lines derived from the commonly used *Arabidopsis* strains Col-0 and L*er*. Although we identified several cases in which AGO1 buffered genetic variation, none of the *AGO1*-dependent loci overlapped with those buffered by HSP90 for the traits assayed. We focused on 1 buffered locus where *AGO1* perturbation uncoupled the traits days to flowering and rosette leaf number, which are otherwise closely correlated. Using a bulk segregant approach, we identified a nonfunctional L*er hua2* mutant allele as the causal AGO1-buffered polymorphism. Introduction of a nonfunctional *hua2* allele into a Col-0 *ago1* mutant background recapitulated the L*er*-dependent *ago1* phenotype, implying that coupling of these traits involves different molecular players in these closely related strains. Taken together, our findings demonstrate that even though AGO1 and HSP90 buffer genetic variation in the same traits, these robustness regulators interact epistatically with different genetic loci, suggesting that higher-order epistasis is uncommon.

Plain Language Summary

Argonaute 1 (AGO1), a key player in plant development, interacts with the chaperone HSP90, which buffers environmental and genetic variation. We found that *AGO1* buffers environmental and genetic variation in the same traits; however, AGO1-dependent and HSP90-dependent loci do not overlap. Detailed analysis of a buffered locus found that a nonfunctional *HUA2* allele decouples days to flowering and rosette leaf number in an AGO1-dependent manner, suggesting that the AGO1-dependent buffering acts at the network level.

Keywords: AGO1; HSP90; HUA2; buffering; capacitors; epistasis; Plant Genetics and Genomics

Introduction

Genetic networks rely on various types of feedback loops, redundancy, and other mechanisms like chaperones and small RNAs to ensure phenotypic robustness in spite of environmental or genetic perturbations (Rutherford and Lindquist 1998; Queitsch *et al.* 2002; Masel and Siegal 2009; Whitacre 2012; Lempe *et al.* 2013; Lachowiec *et al.* 2018; Zabinsky *et al.* 2019). Network disruptions decrease environmental and developmental robustness and, dependent on their nature, increase phenotypic variation in a trait or affect organismal phenotypes more broadly. For example, perturbation of the essential chaperone HSP90 broadly increases phenotypic variation in plants, fungi, and animals, with many organismal traits affected in a background-specific manner (Rutherford and Lindquist 1998; Queitsch *et al.* 2002; Yeyati *et al.* 2007; Sangster, Salathia, Lee, *et al.* 2008; Sangster, Salathia, Undurraga, *et al.* 2008; Jarosz and Lindquist 2010; Rohner *et al.* 2013; Karras *et al.* 2017; Zabinsky *et al.* 2019). When fully functional, HSP90 chaperones a select but highly diverse group of client proteins, including many kinases, receptors and transcription factors with crucial roles in development (Schopf *et al.* 2017). When chaperone function is perturbed, client proteins encoding genetic variants may fail to mature or fold differently, leading to pathway failure or rewiring (Dorrity *et al.* 2018) and hence altered phenotypes (Zabinsky *et al.* 2019). The phenomenon that HSP90 keeps genetic variation phenotypically silent and HSP90 perturbation allows its expression has become known as phenotypic capacitance (Rutherford and Lindquist 1998; Masel and Siegal 2009) – a different term for epistasis (Zabinsky *et al.* 2019). In

Received: June 27, 2022. **Accepted:** October 18, 2022

contrast to the traditional definition of epistasis, which describes the nonreciprocal interaction of 2 loci, phenotypic capacitance is an epistasis phenomenon in which 1 locus, e.g. *HSP90*, interacts with several others. HSP90 perturbation can increase phenotypic variation even in the absence of genetic variation, presumably because subtle differences in microenvironment, developmental stage, or cell state lead to the inhibition of different client proteins among individuals in a seemingly stochastic manner (Zabinsky *et al.* 2019).

Another important source of developmental and environmental robustness is posttranscriptional regulation by small RNAs. Small RNAs regulate the expression of their target genes in a sequence-specific manner. In plants, most endogenous posttranscriptional gene regulation is mediated by AGO1 loaded with microRNAs (miRNAs, MIR) (Axtell 2013; Bologna and Voinnet 2014). In animals, some miRNAs are known to buffer stochastic (Hilgers *et al.* 2010), environmental (Li *et al.* 2009), and genetic variation (Cassidy *et al.* 2013). miRNAs play major roles throughout plant development, including in the onset of flowering, an irreversible developmental transition of outsized effect on reproductive success in annual plants (Dong *et al.* 2022). In particular, the MIR156 and MIR172 gene families are essential for fine-tuning expression of the complex gene network that determines the number of days until flowering is initiated and the number of rosette leaves at this developmental stage. Misregulation or mutation of their gene targets alters both traits in the crucifer model *Arabidopsis thaliana* (Aukerman and Sakai 2003; Yamaguchi *et al.* 2009; Wu *et al.* 2009).

In *Arabidopsis*, the traits days to flowering (i.e. flowering time, onset of flowering) and rosette leaf number are so closely linked that the traits are often used interchangeably. This close correlation reflects the need for sufficient vegetative tissue (i.e. rosette leaves) to produce the resources for flowering and seed development. Because of the irreversible nature of the transition from the vegetative to the reproductive stage in *Arabidopsis*, the coupling of these traits is crucial for reproductive success. *Arabidopsis* mutants that flower with as few as 3 or 4 adult leaves develop very few seeds and often show weakened growth habits (Soppe *et al.* 1999; Gómez-Mena *et al.* 2001). Uncoupling of flowering time and rosette leaf number occurs in some early and late flowering time mutants (Pouteau *et al.* 2004; Rival *et al.* 2014) and in response to treatment with nitrogen dioxide (Takahashi and Morikawa 2014); however, the mechanistic underpinnings for this uncoupling remain unknown.

Studies in several organisms suggest that AGO proteins are chaperoned by HSP90. HSP90 physically interacts with AGO proteins in yeast (Wang *et al.* 2013; Okazaki *et al.* 2018), flies (Iwasaki *et al.* 2010; Miyoshi *et al.* 2010; Gangaraju *et al.* 2011), humans (Johnston *et al.* 2010; Gangaraju *et al.* 2011), *Tetrahymena* (Woehrer *et al.* 2015), and plants (Iki *et al.* 2010, 2012). Because miRNAs buffer environmental and genetic perturbations and AGO1 interacts with HSP90, we set out to investigate the extent to which *AGO1* perturbation affects phenotypic variation in isogenic *Arabidopsis* seedlings and buffers genetic variation in divergent backgrounds, and *AGO1*-dependent loci overlap with HSP90-dependent loci. We find that *AGO1* perturbation can significantly increase phenotypic variation in morphological and quantitative traits in isogenic seedlings. *AGO1* perturbation also buffers the phenotypic effects of genetic variation between 2 divergent backgrounds. However, none of the AGO1-buffered loci overlapped with those buffered by HSP90, consistent with a prevalence of first-order epistatic interactions relative to higher-order epistasis. Lastly, our detailed investigation of 1 such buffered locus reveals that the coupling of the fitness-relevant traits days to flowering and rosette leaf number relies on different molecular players in these commonly used strains of *Arabidopsis*.

Materials and methods

Plant materials and growth conditions

The following parental lines were used: Col-0, *ago1-27* in the Col-0 background, and Stepped Aligned Inbred Recombinant Strains (STAIRS) N9448, N9456, N9472, N9501 (Morel 2002; Koumproglou *et al.* 2002). *ago1-27* plants were crossed into the STAIR lines and F_2's that carried the wild-type and *ago1-27* allele in both Col-0 and the STAIRS backgrounds were isolated. Selected F_2's and their progeny were used to perform the described experiments. For the hypocotyl and root length assays, the plants were grown on MS media containing 0.0005% MES hydrate, 0.004% vitamin solution, 3% phytoagar, and 1% sucrose.

Genotyping of F_2 plants

We used PCR to genotype the F_2's from each STAIRS—*ago1-27* cross. PCR conditions for *ago1-27* genotyping is as follows: 5′ at 94°C, followed by 35 cycles at 30 s at 94°C, 30 s at 55°C, 1 min at 72°C. PCR product was then digested at 37°C with Bsp1286I, which cuts wild-type sequence. PCR conditions for MIR156F genotyping is as follows: 2′ at 95°C, followed by 35 cycles at 30 s at 94°C, 50 s at 57°C, and 40 s at 72°C.

Hypocotyl and root length assays

Seeds from different genotypes were plated on agar plates (10 seeds/per plate, equally spaced). The plates were stacked in racks to ensure vertical position, wrapped in aluminum foil, and transferred to 4°C for 5 days to promote germination. They were then unwrapped and exposed to light for 2 h. After that, the plates were wrapped in aluminum foil again, to prevent further light exposure, and were transferred to a 23°C tissue culture incubator for 7 days. The plants were grown vertically. After that, the plates were taken out and photographed. The photographs were used to measure the seedlings' hypocotyls and roots using the ImageJ software (http://rsbweb.nih.gov/ij/).

Early morphology traits analysis

Seeds from the different genotypes were plated on agar (36 seeds/per plate). The plates were wrapped in aluminum foil and transferred to 4°C for 5 days. Plates were unwrapped and transferred to long days (LD) in 23°C tissue culture incubator for 10 days. The plants were grown horizontally. The plates were rotated every day to prevent biases due to location in the incubator. On the 10th day, the seedlings were scored for their morphological traits.

Flowering time experiments

Seeds from different genotypes were embedded in 1 ml of 0.1% agar and then stratified for 5 days at 4°C. They were sown on soil in 36-pot trays. Flowering time was measured by scoring both the number of rosette leaves and days to flowering when the primary inflorescence of the plant had reached a height of 1 cm. Flowering time experiments were performed in LD (16 h of light, 8 h of dark), at 23°C.

Rosette diameter measurements

The diameter of the rosette was measured on the day that the primary inflorescence of the plant reached a height of 1 cm.

Vernalization treatment

Seeds were stratified for 5 days at 4°C and then sown on soil. They were allowed to grow for 5 days at 23°C in LD or short days (SD) conditions and then transferred to 4°C for 40 days, according to recommendations from Sung et al. (2006).

Gene expression analysis

To determine the expression levels via qPCR, total RNA was isolated from the aerial parts of 14-day old plants at ZT16 using the SV Total Isolation System (Promega). RNA quality was determined using a Nanodrop and only high-quality samples (A260/A230 > 1.8 and A260/A280 > 1.8) were used for subsequent qPCR experiments. To remove possible DNA contamination, RNA was treated with DNaseI (Ambion) for 60 min at 37°C. We used the Transcriptor First Strand cDNA Synthesis Kit (Roche) for cDNA synthesis. The qPCR primers were designed using the Universal Probe Library Assay Design Center tool (Roche), and Primer3 (Untergasser et al. 2012). Specific amplification was confirmed before conducting the qPCR experiments. The qPCR experiments were carried out in 96-well plates with a LightCycler480 (Roche) using SYBR green. The following program was used for the amplification: predenaturation for 5 min at 95°C, followed by 35 cycles of denaturation for 15 s at 95°C, annealing for 20 s at 55°C, and elongation for 30 s at 72°C. All qPCR experiments were carried out with 2 biological replicates (independent samples harvested on different days) and with 3 technical replicates per sample.

RNA-seq samples were prepared similarly as for qPCR, and then using the Illumina stranded Tru-seq kit following the standard protocol. Samples were sequenced using the Nextseq550 platform. We used TopHat (v2.1.2) to align RNA-seq reads to the TAIR10 genome annotation (Trapnell et al. 2009), htseq-count (v0.12.4) to calculate counts per gene (Anders et al. 2015), using a minimum map quality of 10 and Cuffdiff (v2.2.1) to generate FPKMs (Trapnell et al. 2013), and DESeq2 to identify differentially expressed genes among genotypes (Love et al. 2014).

Sequencing of miR156F, D, and E in diverse *A. thaliana* strains

The genes *MIR156F*, *MIR156D*, and *MIR156E* were amplified using the primers listed in Supplementary Table 7. PCR products were sequenced by the Sanger method. The sequences were aligned using T-coffee.

Bulk segregant analysis—library preparation and sequencing

Approximately 400 F_2 plants were sown, and leaf samples of equal size were collected from 100 plants that resembled the STAIRS9472; *ago1-27* phenotype (6 leaves or fewer at flowering) and 100 plants with a greater number of leaves. Individual plants were genotyped. In parallel, leaf samples were collected for all genotypes. DNA was extracted using CTAB extraction (Weigel and Glazebrook 2002) and quantified using the Qubit HS dsDNA assays. Libraries were quality checked on the Agilent 2100 bioanalyzer using a DNA 1000 chip (Agilent). Samples were pooled and libraries were generated using the Nextera sample kit according to the manufacturer's instruction. DNA concentration of the amplified libraries was measured with the DNA 1000 kit as well as the DNA high-sensitivity kit for diluted libraries (both Agilent). Samples were sequenced on an Illumina Nextseq in a 75-bp paired-end run.

Bulk segregant analysis—data analysis

Using the function SHORE import, raw reads were trimmed or discarded based on quality values with a cutoff Phred score of +38. After correcting the paired-end alignments with an expected insert size of 300 bp, we applied SHORE consensus to identify variation among mutants and reference. We applied SHOREmap using the included *Ler*/Col-0 SNPs. Plot boost was applied to further define a mapping interval.

Results

Genetic perturbation of *AGO1* increases phenotypic variation in isogenic *Arabidopsis* seedlings

To determine if perturbation of *AGO1* leads to increased phenotypic variation in isogenic seedlings, we examined several morphological and quantitative traits of 2 hypomorphic *ago1* mutants, *ago1-46* (Smith et al. 2009), and *ago1-27* (Morel 2002), the former being a less severe mutant than the latter. Ten-day old isogenic seedlings of *ago1-46* and *ago1-27* showed increased phenotypic variation in morphological traits, such as lesions in cotyledons (Mason et al. 2016), rosette symmetry, and organ defects, compared to isogenic wild-type seedlings (Fig. 1 and Supplementary Table 1). As expected, the more severe *ago1-27* mutant showed more abnormal phenotypes than the less severe *ago1-46* mutant. Next, we examined hypocotyl length in the dark, a quantitative trait that shows increased variation in response to HSP90 perturbation (Queitsch et al. 2002; Sangster, Salathia, Undurraga, et al. 2008). Similar to our previous results (Queitsch et al. 2002; Sangster, Salathia, Undurraga, et al. 2008), *ago1-27* dark-grown seedlings showed a different mean value ($P < 2.3e^{-16}$, Wilcoxon test) and significantly greater variance of hypocotyl length than wild-type seedlings ($P = 0.0002$, Levene's test) (Fig. 1b and Supplementary Table 1). The less severe *ago1-46* seedlings also showed a different mean value (P-value $= 3.6e^{-05}$, Wilcoxon test) and greater variance of hypocotyl length compared to wild-type seedlings (P-value = 0.00004, Levene's test). Based on these results, AGO1 maintains phenotypic robustness and buffers developmental noise among isogenic seedlings in a manner similar to HSP90.

AGO1 buffers genetic variation independent of HSP90

We next tested whether *AGO1* perturbation could reveal cryptic genetic variation and whether *AGO1*-dependent loci overlapped with those buffered by *HSP90*. To do so, we introgressed the hypomorphic *ago1-27* allele into Col-0 lines with single chromosome substitutions from another, genetically divergent *Arabidopsis* strain, Landsberg *erecta* (*Ler*) (STAIRS, STepped Aligned Inbred Recombinant Strains, Fig. 2a and Supplementary Table 2). STAIRS lines have been generated for chromosomes 1, 3, and 5 (Koumproglou et al. 2002). Since *AGO1* is located on chromosome 1, we excluded these STAIRS lines from our analysis. For chromosomes 3 and 5, we selected 2 STAIRS lines each (chr3; N9448 and N9459, chr5; N9472 and N9501). The introgressed lines were genotyped to confirm the integrity of the respective *Ler* segments.

We measured hypocotyl and root length, rosette diameter, and the closely correlated traits days to flowering and rosette leaf number across many individual plants per line using a randomized experimental design (Supplementary Table 2). We selected these traits because they are readily measurable and show evidence of HSP90-buffered variation in our previous studies of Col-0/*Ler* mapping lines (Sangster, Salathia, Lee, et al. 2008; Sangster, Salathia,

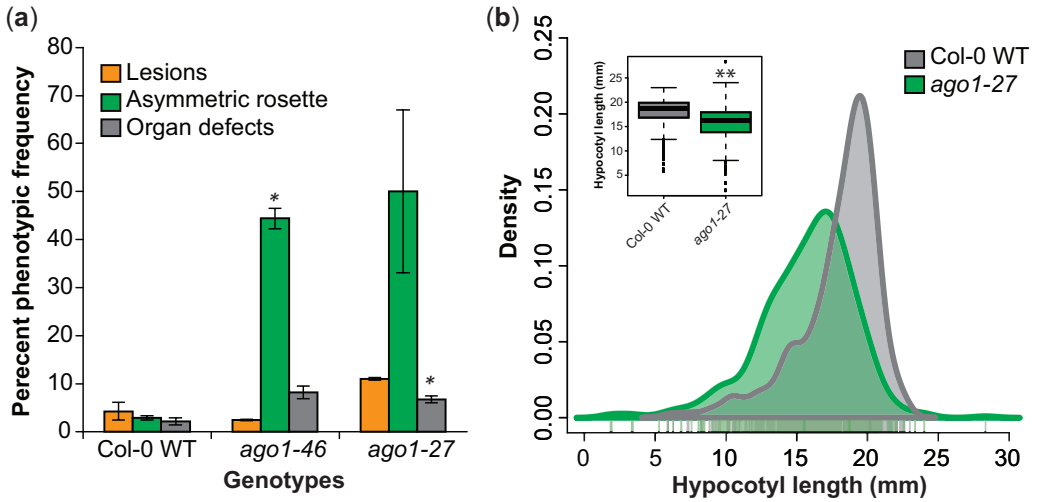

Fig. 1. Perturbation of AGO1 increases phenotypic variation among isogenic seedlings. a) Early seedling trait measures for wild-type (Col-0 WT), *ago1-46*, and *ago1-27* seedlings. Ten-day-old seedlings were scored for 3 different morphological traits: lesions, asymmetrical rosettes, and organ defects. The data represent 2 biological replicates (2 replicates, $n = 144$ for *ago1* mutants and $n = 216$ for Col-0 WT, $^{*}P < 0.05$, ttest). b) Hypocotyl mean length and variance differ between wild-type and *ago1*-mutant seedlings. Hypocotyl length was measured for 7-day old, dark-grown seedlings. *ago1-27* mutant seedlings showed greater variance than Col-0 wild-type seedling in hypocotyl length (Levene's test, $P < 1.0E{-}03$; $n = 475$ for *ago1-27*, $n = 486$ for Col-0 WT). Inset: boxplots of hypocotyl length means. Y-axis represents hypocotyl length (mm), $^{**}P < 1.0E{-}15$, Mann–Whitney Wilcoxon test.

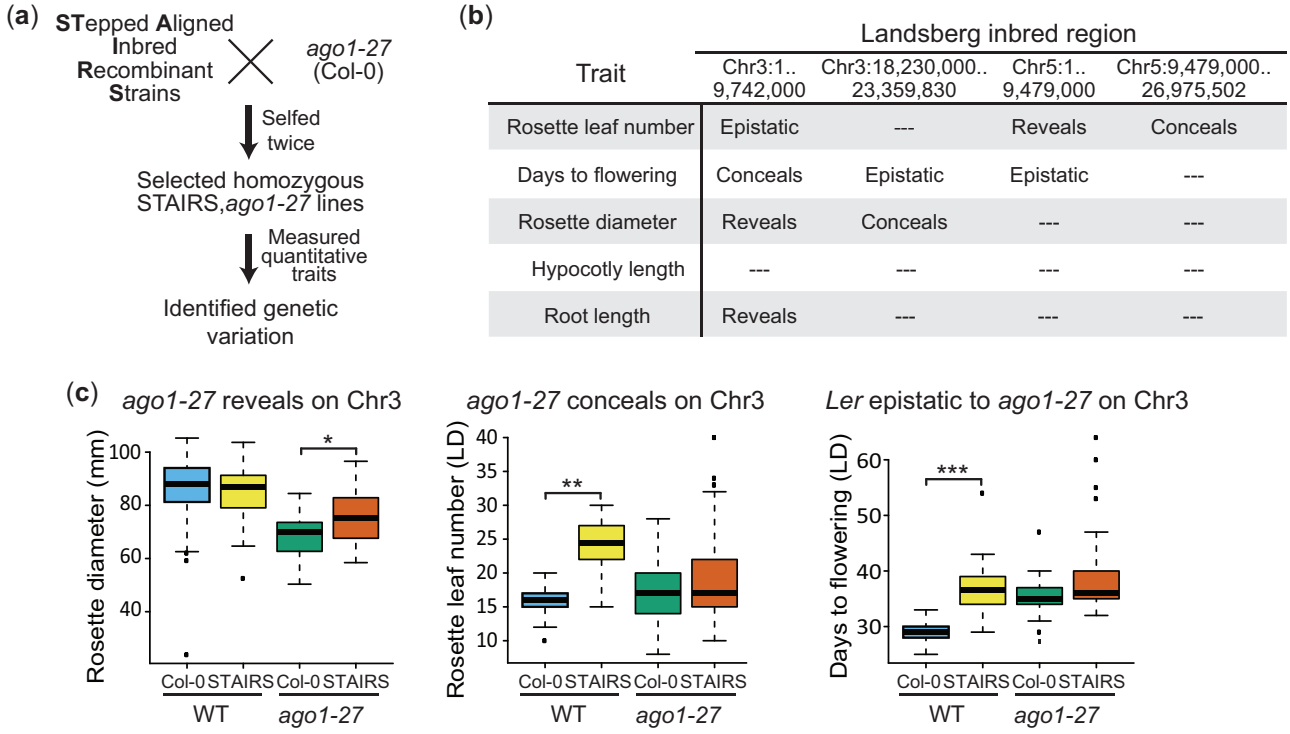

Fig. 2. Perturbation of AGO1 buffers genetic variation. a) Experimental design to examine the phenotypic consequences of genetic variation within the STAIRS in the context of the *ago1-27* mutation. b) Summary of examined quantitative traits with evidence for *AGO1*-dependent or *Ler*-dependent variation in each tested STAIRS line. AGO1 perturbation reveals a cryptic genetic variant if this variant's contribution to a quantitative trait can be detected only in an *ago1*-mutant background. AGO1 perturbation conceals a genetic variant if this variant's contribution to a quantitative trait can no longer be detected in an *ago1*-mutant background. Genetic variation in the respective *Ler* segments can epistatically interact (i.e. mask) the phenotypic differences observed between Col-0 wild-type seedlings and *ago1-27* mutant seedlings in the Col-0 background. For STAIRS line N9472, 78 seedlings were measured for hypocotyl length in the dark; for STAIRS lines N9448, N9459, and N9501, 100 seedlings were measured for this trait. At least 32 plants were measured for all other traits. See Supplementary Tables 2 and 3 for trait values and assessment of significance. c) Three examples of *AGO1*-dependent and 1 example of *Ler*-dependent genetic variation are shown for 3 different traits. left, Col-0 WT; left-middle, STAIRS; right-middle, *ago1-27* in the Col-0 background; right, *ago1-27* in a STAIRS background.

Undurraga, *et al.* 2008). Specifically, 3 previously described *HSP90*-dependent loci within the *Ler* segments of the tested STAIRS lines affect the traits measured here (Sangster, Salathia, Lee, *et al.* 2008; Sangster, Salathia, Undurraga, *et al.* 2008).

AGO1 perturbation may alter the contribution of a cryptic genetic variant to a quantitative trait in 2 ways: first, *AGO1* perturbation may reveal a genetic variant by increasing its contribution to a trait or, second, *AGO1* perturbation may conceal a genetic

variant by increasing the relative contribution of others. Indeed, the phenomenon of revealing and concealing genetic variation has been previously observed for HSP90 perturbation across many traits in *Arabidopsis* recombinant inbred lines (Sangster, Salathia, Lee, *et al.* 2008). In addition, genetic variation in the respective *Ler* segments may mask the phenotypic differences observed between Col-0 wild-type and the *ago1-27* mutant that was generated in the Col-0 background (i.e. *Ler* segments may epistatically interact with *ago1-27*). We observed all 3 scenarios of epistasis (Fig. 2, b and c and Supplementary Figs. 2 and 3). Despite the strong evidence that HSP90 facilitates AGO1 function in many organisms, including plants, no overlap of *AGO1*-dependent loci with HSP90-dependent loci was observed.

Perturbation of *AGO1* uncouples flowering time and rosette leaf number in a background-specific manner

One AGO1-buffered locus showed dramatically different effects on the 2 closely correlated traits days to flowering and rosette leaf number (Fig. 3, a–c). *Arabidopsis* plants develop about 1 rosette leaf per day until flowering is initiated. On average, Col-0 wild-type plants initiated flowering ∼5 days later and have ∼5 more leaves than the STAIRS line 9472 that carries a *Ler* segment on chromosome 5 (coordinates 1–9,479,000 bp). This result was expected because the *Ler* segment in this STAIRS line encompasses the *FLOWERING LOCUS C (FLC)* gene (Fig. 3d) which is nonfunctional in the *Ler* strain (Michaels *et al.* 2003; Liu *et al.* 2004). *FLC* is a strong repressor of flowering (Whittaker and Dean 2017). In the Col-0 background, *ago1-27* plants initiated flowering ∼9 days later and have ∼2 more leaves, albeit the traits were less tightly correlated than in wild type (Fig. 3c, compare blue and green dots). In stark contrast, in the STAIRS9472 background, *ago1-27* plants showed no change in the number of days to flowering; however, these plants showed dramatically fewer leaves at the onset of flowering, developing on average only ∼4 leaves. In fact, the severity of the rosette leaf number phenotype of STAIRS9472; *ago1-27* was comparable to that observed in loss-of-function early flowering mutants (Pouteau *et al.* 2004; Undurraga *et al.* 2012). In short, *AGO1* perturbation in the STAIRS line specifically affected the trait rosette leaf number while not affecting the trait days to flowering.

The close correlation of the traits days to flowering and rosette leaf number traits relies on *FLC* in the Col-0 background

The *Ler* fragment in STAIRS9472 encompasses several known flowering time genes, including *FLC* which delays flowering by repressing the gene *FLOWERING LOCUS T (FT)*. *FLC* expression is repressed when plants are exposed to cold temperatures for a prolonged period of time (i.e. vernalization or winter period), allowing *FT* expression and onset of flowering (Andrés and Coupland 2012; Whittaker and Dean 2017). Genetic variation in *FLC* and in *FRIGIDA (FRI)*, a positive regulator of *FLC*, accounts for the vast majority of differences in flowering time across *Arabidopsis* strains (Shindo *et al.* 2005; Kim *et al.* 2009; Bloomer and Dean 2017). Many *Arabidopsis* strains do not require vernalization to initiate flowering because they carry *FLC* mutations, as is the case for *Ler*, or *FRI* mutations, as is the case for Col-0. The STAIRS9472 line carries the nonfunctional *Ler FLC* allele.

We wondered if the lack of functional *FLC* in STAIRS9472; *ago1-27* contributed to its unusual phenotype. To test this possibility, we examined the consequences of repressing *FLC* through vernalization for both flowering time traits in Col-0 wild-type, STAIRS9472, Col-0 *ago1-27*, and STAIRS9472; *ago1-27* plants (Supplementary Fig. 3). Vernalization did not erase the difference in rosette leaf number between Col-0 *ago1-27* and STAIRS9472; *ago1-27* plants, with the latter still showing significantly fewer leaves ($P = 5.704e^{-12}$ Wilcoxon test). However, vernalization uncoupled both flowering time traits in an *AGO1*-dependent manner in the Col-0 background. Although vernalized *ago1-27* plants initiated flowering ∼5 days later than vernalized Col-0 wild-type plants, they had ∼4 fewer leaves rather than more leaves. We conclude that the close association of days to flowering and rosette leaf number in the Col-0 background requires the presence of functional *FLC* and *AGO1*. Perturbation of *AGO1* alone diminished the close correlation between both traits but did not reverse it. *Ler* and other natural *FLC* mutants must have rewired flowering time pathways such that the traits days to flowering and rosette leaf number remain closely correlated in the absence of functional *FLC*.

MIR156 polymorphisms are unlikely to cause *AGO1*-dependent phenotype

To identify the causal polymorphism(s) underlying the *AGO1*-dependent STAIRS9472 phenotype, we examined other genes within the *Ler* segment with functions in flowering time (Song *et al.* 2013, 2015; Spanudakis and Jackson 2014) and candidate polymorphisms between Col-0 and *Ler* (Nordborg *et al.* 2005; Borevitz *et al.* 2007; Ossowski *et al.* 2008) (Fig. 3d). We measured expression of these candidate genes among the 4 genotypes: Col-0 wild-type, STAIRS9472, Col-0 *ago1-27* and STAIRS9472; *ago1-27*; for the 3 *MIR156* genes (e, d, f), and *MIR172b*, we measured expression of major target genes (Ji *et al.* 2011). As expected, *FLC* expression was barely detectable in STAIRS9472 and STAIRS9472; *ago1-27* plants (Fig. 3d), consistent with the known disruption of *FLC* in *Ler* (Michaels *et al.* 2003; Liu *et al.* 2004). *FLC* expression increased in Col-0 *ago1-27* plants relative to Col-0 wild-type plants, consistent with the late flowering phenotype of the former genotype. As a general trend, target genes of *MIR156* increased in expression in the STAIRS *ago1-27* background compared to target gene expression in the Col-0 *ago1-27* background, suggesting that *MIR156* may be less functional in the STAIRS line. *MIR156* represses the expression of several *SQUAMOSA PROMOTER BINDING LIKE* (SPL) transcription factors (miR156-SPL module, Figs. 3e and 5d) that regulate flowering by activating and repressing other transcription factors and miRNAs (Aukerman and Sakai 2003; Yamaguchi *et al.* 2009; Wu *et al.* 2009). Overexpression of *MIR156* leads to delayed onset of flowering with many more rosette leaves (Wu *et al.* 2009; Xu *et al.* 2016), suggesting that less functional *MIR156* may diminish rosette leaf number.

We searched for *Ler*-specific polymorphisms in the *MIR156* genes in available genome assemblies and found a predicted single-nucleotide polymorphism (SNP) within the loop of *MIR156f*. Resequencing of all 3 *MIR156* genes confirmed this SNP and identified an additional deletion of 14 nucleotides near the base of the stem loop. As the *MIR156* genes are highly conserved in the plant kingdom (Cuperus *et al.* 2011; Luo *et al.* 2013), we examined their natural variation among other *Arabidopsis* strains, sequencing an additional 55 strains. Of all sequenced strains, 42 carried the *Ler*-specific C-to-T SNP, 1 carried a C-to-G SNP, and 32 carried the 14-nt deletion (Supplementary Fig. 2). The presence or absence of the deletion was highly correlated with the presence or absence of the SNP ($R^2 = 0.3506$, $P = 0.0007$, Pearson correlation test). To address whether either 1 or both *Ler*-specific *MIR156f* polymorphisms affect rosette leaf number, we tested for association with this trait across these accessions [phenotypic data from

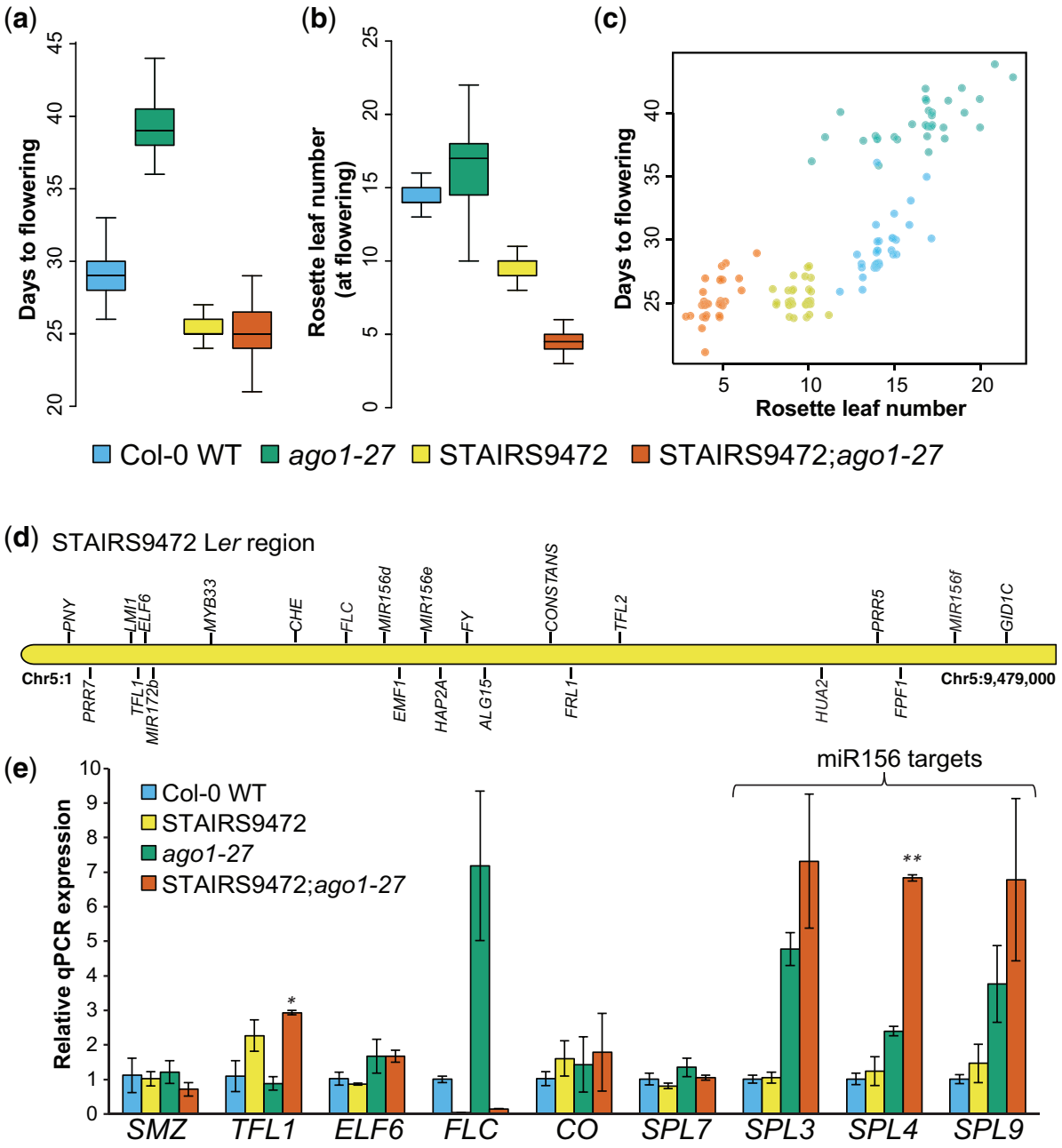

Fig. 3. AGO1 perturbation uncouples the traits days to flowering and rosette leaf number. Plants for Col-0 WT, STAIRS9472, Col-0 *ago1-27*, and STAIRS9472; *ago1-27* were grown in a random block design in LD, $n = 30–36$. Days to flowering were recorded and rosette leaf numbers at the onset of flowering were counted. Blue, Col-0 WT; yellow, STAIRS9472; red, *ago1-27* in the Col-0 background; green, *ago1-27* in the STAIRS9472 background. a) Days to flowering. The *ago-1* mutant flowered ~9 days later than Col-0 WT ($P = 5.51E{-}12$, Mann–Whitney Wilcoxon test); no significant difference was found between STAIRS9472 and the *ago-1* mutant in the STAIRS9472 background ($P = 0.4714$, Mann–Whitney Wilcoxon test). The *Ler* introgression in STAIRS9472 was epistatic to *ago1-27*, $^{*}P < 0.0001$, Mann–Whitney Wilcoxon test. b) Rosette leaf number. Col-0 WT plants showed fewer leaves than *ago1-27* mutant plants, consistent with the mutant's late flowering phenotype. In the STAIRS9472 background, *ago1-27* mutant plants showed no change in the number of days to flowering; however, these plants developed significantly fewer leaves ($P = 3.45E{-}12$, Mann–Whitney Wilcoxon test). c) Scatter plot of the 2 measured traits days to flowering and rosette leaf number in the 4 tested genotypes. The traits were less well correlated in the *ago-1* mutant in the Col-0 background (compare blue and green dots); however, the normally tight correlation was fully lost in the STAIRS background (compare red and yellow dots). d) Known flowering time genes are residing within the *Ler* chromosome 5 region of the STAIRS9472 line. e) Quantitative PCR measurements for candidate gene expression. *TFL1* and *SPL4* were significantly increased in expression in the STAIRS9472; *ago1-27* background. Fourteen-day-old plant tissue was collected at ZT16 (Zeitgeber 16; 16 h after dawn). Mean expression data represent 2 biological replicates, each with 3 technical replicates. Standard error is indicated ($^{*}P < 0.05$, $^{**}P < 0.005$, *T*-test).

Lempe *et al.* (2005)]. No association was found. Although this result did not rule out the *MIR156f* polymorphisms as the causative *AGO1*-dependent alleles, it made it less likely that these polymorphisms would explain the unusual STAIRS9472; *ago1-27* phenotype.

Identifying the *AGO-1*-dependent *Ler*-specific polymorphism with a bulk segregant analysis

To identify the *Ler*-specific variant(s) causing the observed trait uncoupling in STAIRS9472; *ago1-27* plants, we used a classic bulk segregant analysis followed by high-throughput sequencing

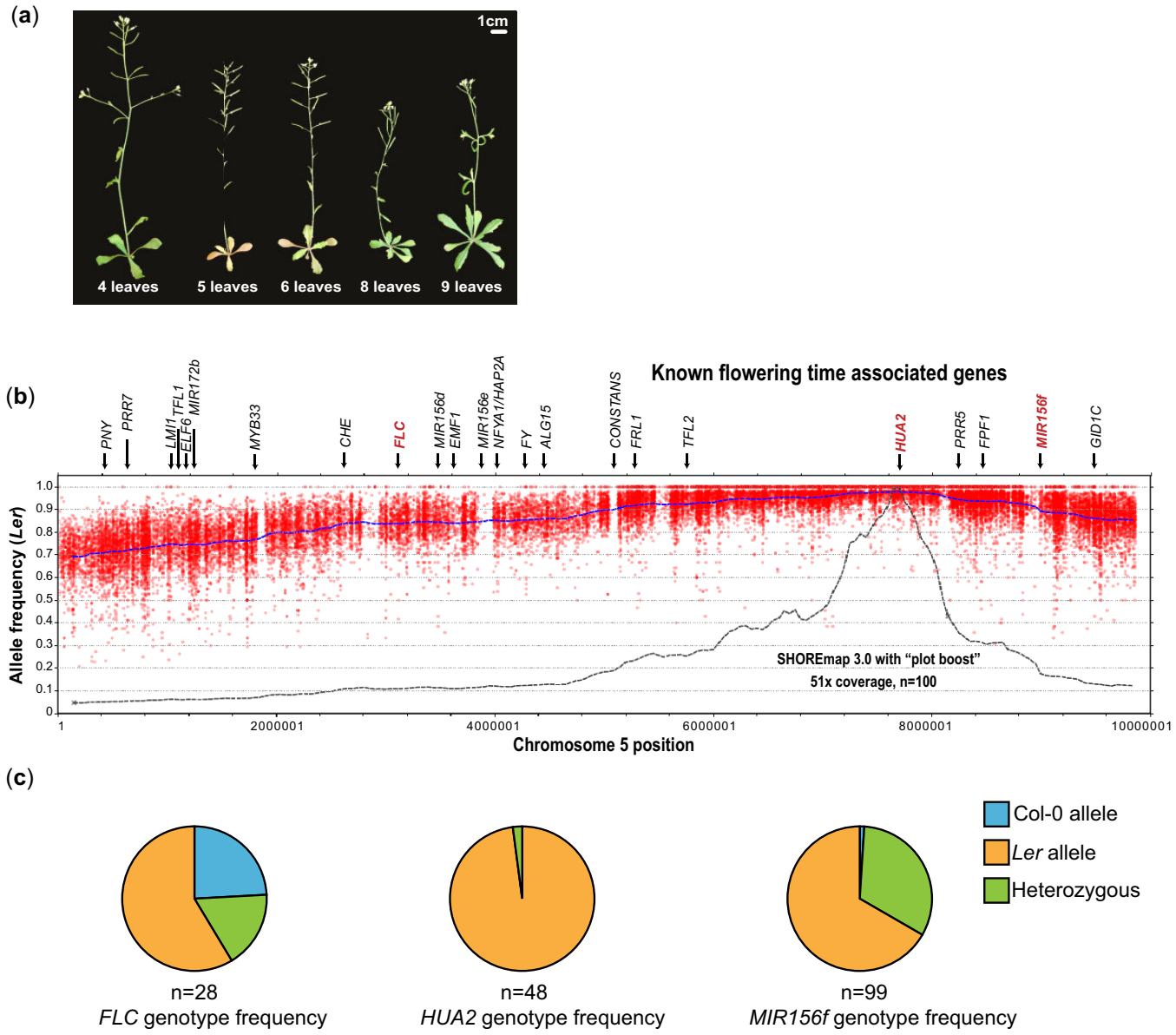

Fig. 4. Bulk segregant analysis identifies the nonfunctional *Ler hua2* allele as a candidate *AGO1*-dependent locus. a) F_2 plants from *ago1-27* × STAIRS9472 cross were grown in LD, phenotypes were recorded, and plants were genotyped for the *ago1-27* allele. For bulk segregant analysis, we selected plants that were homozygous for the *ago1-27* mutation and flowered with 6 or fewer leaves ($n = 100$), resembling the *AGO1*-dependent STAIRS9472 phenotype. Representative F_2 *ago1-27* plants at flowering are shown. Scale bar = 1 cm. b) Bulk segregant analysis. Red dots represent *Ler*-allele frequencies on chromosome 5 (bp, x-axis). Allele frequencies (y-axis) were estimated as the fraction of reads supporting a *Ler* allele divided by the number of reads mapping to that locus. Dashed blue line represents sliding window-based allele frequencies as estimated by SHOREmap. Dashed black line represents window-based plot boost as estimated by SHOREmap. The *Ler hua2-5* allele emerged as the candidate *AGO1*-dependent locus because *Ler*-allele frequencies were highest at this locus compared with other regions on chromosome 5. d) F_2 plants homozygous for the *ago1-27* mutation with 6 or fewer leaves at flowering were PCR genotyped for alleles at *FLC*, *HUA2*, and *MIR156f* loci. The near perfect enrichment of *Ler hua2-5* allele validates the result of our bulk segregant analysis.

(Cuperus *et al.* 2010; Sun and Schneeberger 2015). To generate a segregating population for the tested alleles, we crossed STAIRS9472 with *ago1-27* and allowed for selfing to generate F_2 seeds. F_2 plants were measured for days to flowering and the number of rosette leaves at this point (Fig. 4a). From this F_2 experiment, we pooled plants based on phenotype, defining the STAIRS9472; *ago1-27* phenotype as plants with 6 or fewer rosette leaves (Figs. 3, a–c and 4a) and isolated their DNA. We combined equal DNA amounts for 100 plants with the *AGO1*-dependent STAIRS9472 phenotype and 100 plants with higher numbers of rosette leaves. Using short-read sequencing, we aligned reads to the relevant chromosome 5 segment using SHOREmap (Sun and Schneeberger 2015), relying on the many known polymorphisms between *Ler* and Col-0 to distinguish *Ler*- and Col-0-specific reads. If successful, bulk segregant analysis will show increasing enrichment of homozygosity near the causal locus, with the causal locus at the center of a peak region (Salathia *et al.* 2007; Schneeberger *et al.* 2009; Cuperus *et al.* 2010; Sun and Schneeberger 2015). This mapping approach works best if variation at a single locus causes a segregating phenotype, and if phenotypes can be clearly distinguished from each another in order to pool samples with high confidence.

Although our phenotype of interest was quantitative in nature, i.e. a range of leaf numbers rather than an absence or

presence of a feature, we observed a skew toward L*er* alleles on chromosome 5 with a SHOREmap peak region at chr5:7,600,000 to chr5:7,800,000 (Fig. 4b). Of the known flowering time-associated genes, only 1 fell in this peak region, *HUA2* (AT5G23150). Some L*er* backgrounds, including the STAIRS9742 line, carry a premature stop codon mutation in *HUA2*, likely disrupting function (Chen and Meyerowitz 1999; Doyle *et al.* 2005; Zapata *et al.* 2016). *HUA2* function is less well characterized than that of other flowering time genes; however, *hua2* mutants in a Col-0 background show reduced *FLC* levels and fewer rosette leaves at onset of flowering (Doyle *et al.* 2005). *MIR156f* did not reside in the peak region, consistent with the previously described lack of genotype-phenotype association (Fig. 4, b and c).

To confirm that loss of functional *HUA2* was responsible for the *AGO1*-dependent phenotype in STAIRS9472, we used a Col-0-derived *hua2* mutant allele, *hua2-4*, and generated a double mutant *hua2-4; ago1-27* in the Col-0 background. We predicted that this homozygous double mutant would exhibit the uncoupling of days to flowering and rosette leaf number traits observed in the STAIRS9472; *ago1-27* line. Using a segregating F_2 population, we simultaneously measured days to flowering and rosette leaf number, and genotyped each plant (Fig. 5, a–c). The *hua2-4* single mutant plants and the *hua2-4; ago1-27* double mutant plants showed no significant difference in days to flowering but rosette leaf number was markedly reduced in double mutant plants, recapitulating our original finding with STAIRS9472; *ago1-27* plants. The observed uncoupling of these traits was independent of *FLC* which is not disrupted in the *hua2-4; ago1-27* double mutant. This result suggests that the L*er*-specific, nonfunctional *hua2* allele may compensate for the L*er*-specific *FLC* disruption, thereby maintaining the close association of days to flowering and rosette leaf number traits.

HUA2 effects on gene expression suggest *SPL4* as a likely *HUA2* target

To understand in more detail how *HUA2* affects the complex flowering gene network, we conducted RNA-seq experiments examining wild-type Col-0, single mutants *hua2-4* and *ago1-27* and *hua2-4; ago1-27* double mutant seedlings. As expected, *ago1-27* mutants and Col-0 wild-type showed differential expression of many miRNA target genes (Supplementary Table 6). The expression of the known *HUA2* targets *FLC* and *FLOWERING LOCUS M* (*FLM*, *MAF1*) was reduced in both the single *hua2-4* mutant and the *hua2-4; ago1-27* double mutant seedlings, excluding them as sources of the *AGO1*-dependent phenotype.

However, the comparison of *ago1-27* and *hua2-4; ago1-27* plants showed strong upregulation of *SPL4* expression in the latter (Fig. 5d), consistent with our finding that *SPL4* was strongly upregulated STAIRS9472; *ago1-27* (Fig. 3e). Other important flowering time genes were also differentially expressed in *hua2-4; ago1-27* double mutant plants, including the master regulator *FT*, *LATE ELONGATED HYPOCOTYL(LHY)*, *SUPPRESSOR OF OVEREXPRESSION OF CONSTANS 1 (SOC1)*, *AGAMOUS-LIKE 8 (AGL8, FRUITFUL)*, and *MIR159b* (Fig. 5d). These genes interact in complex ways to control the transition to flowering (Fig. 5e). Because *HUA2* is involved in mRNA processing and splicing (Chen and Meyerowitz 1999; Cheng *et al.* 2003; Janakirama 2013), we speculate that *SPL4* may be one of its targets. *SPL4* has 3 splice isoforms, and 2 of them (*SPL4-2*, *SPL4-3*) lack a miR156-binding site (Yang *et al.* 2012). Overexpression of *SPL4-1*, the splice form with the miR156 binding site, does not affect days to flowering but decreases rosette leaf number. In contrast, overexpression of *SLP4-2* or *SPL4-3* decreases days to flowering and reduces rosette leaf number (Yang *et al.* 2012). In a *hua2; ago1* double mutant background the balance of *SPL4* splice forms may be altered, which together with the absence of functional AGO1 disrupts the close correlation of days to flowering and rosette leaf number.

Discussion

Here we show that AGO1, the principal player in miRNA-mediated control of gene expression in plants, buffers micro-environmental variation and maintains developmental stability in isogenic *Arabidopsis* seedlings. Compared to wild-type Col-0 plants, *ago1* mutant seedlings showed more lesions on cotyledons (Mason *et al.* 2016), more rosette symmetry defects and abnormal organs, and increased variation in hypocotyl length of dark-grown seedlings. Given the crucial role that miRNAs play in plant development, these results are not altogether surprising. miRNAs can impact developmental stability, i.e. the accuracy with which a given genotype produces a trait in a particular environment, in various ways (Hornstein and Shomron 2006; Voinnet 2009). For example, miRNAs can buffer gene expression noise as part of incoherent feedforward loops, in which a transcription factor will activate both the expression of a target gene X and a miRNA, with the latter repressing target gene X (Hornstein and Shomron 2006; Voinnet 2009). miRNAs enforce developmental patterning decisions through mutual exclusion and spatial or temporal restrictions in expression, e.g. by suppressing fate-associated transcription factors in neighboring cells or at a certain time in development (Hornstein and Shomron 2006; Voinnet 2009).

In plants, we previously reported increased variation for the same traits in isogenic seedlings upon perturbation of the chaperone HSP90 (Queitsch *et al.* 2002; Sangster, Salathia, Undurraga, *et al.* 2008), consistent with the reported functional relationship of HSP90 and AGO1 (Iki *et al.* 2010, 2012; Iwasaki *et al.* 2010, 2015; Naruse *et al.* 2018). An exception was the peculiar environmentally-responsive lesions found on cotyledons in *ago1-27* seedlings (Mason *et al.* 2016). *HSP90* single mutants produce far fewer seedlings with lesions than *ago1-27* mutants, and double mutants show many more lesions than *ago1-27* single mutants, inconsistent with simple epistasis. Thus, we previously suggested that AGO1 is a major, but largely HSP90-independent, factor in providing environmental robustness to plants.

In addition to maintaining developmental stability, HSP90 buffers genetic variation in plants, fungi, and animals, including humans (Zabinsky *et al.* 2019). The hypothesized mechanism by which HSP90 overcomes the presence of genetic variation is the chaperone's well-characterized function in protein folding and maturation (Sangster *et al.* 2004; Jarosz *et al.* 2010; Zabinsky *et al.* 2019). This hypothesis is supported by the reported differences among disease-associated protein variants chaperoned by HSP90 vs those chaperoned by HSP70 (Karras *et al.* 2017). Moreover, across thousands of humans, kinases that are HSP90 clients tend to carry more amino acid variants than nonclient kinases, and these amino acid variants are predicted to be more damaging to protein folding (Lachowiec *et al.* 2015).

In contrast, it is harder to envision a simple, direct mechanism by which AGO1 overcomes the presence of genetic variation in either miRNAs or their targets, unless such buffering involves AGO1's close relationship with HSP90 for the latter. Although we observed several instances in which AGO1 perturbation revealed and concealed genetic variation in the same traits in which we previously found HSP90-dependent variation (Sangster, Salathia, Undurraga, *et al.* 2008), there was no overlap in the genetic loci buffered by AGO1 and HSP90. While this result was consistent with our study of

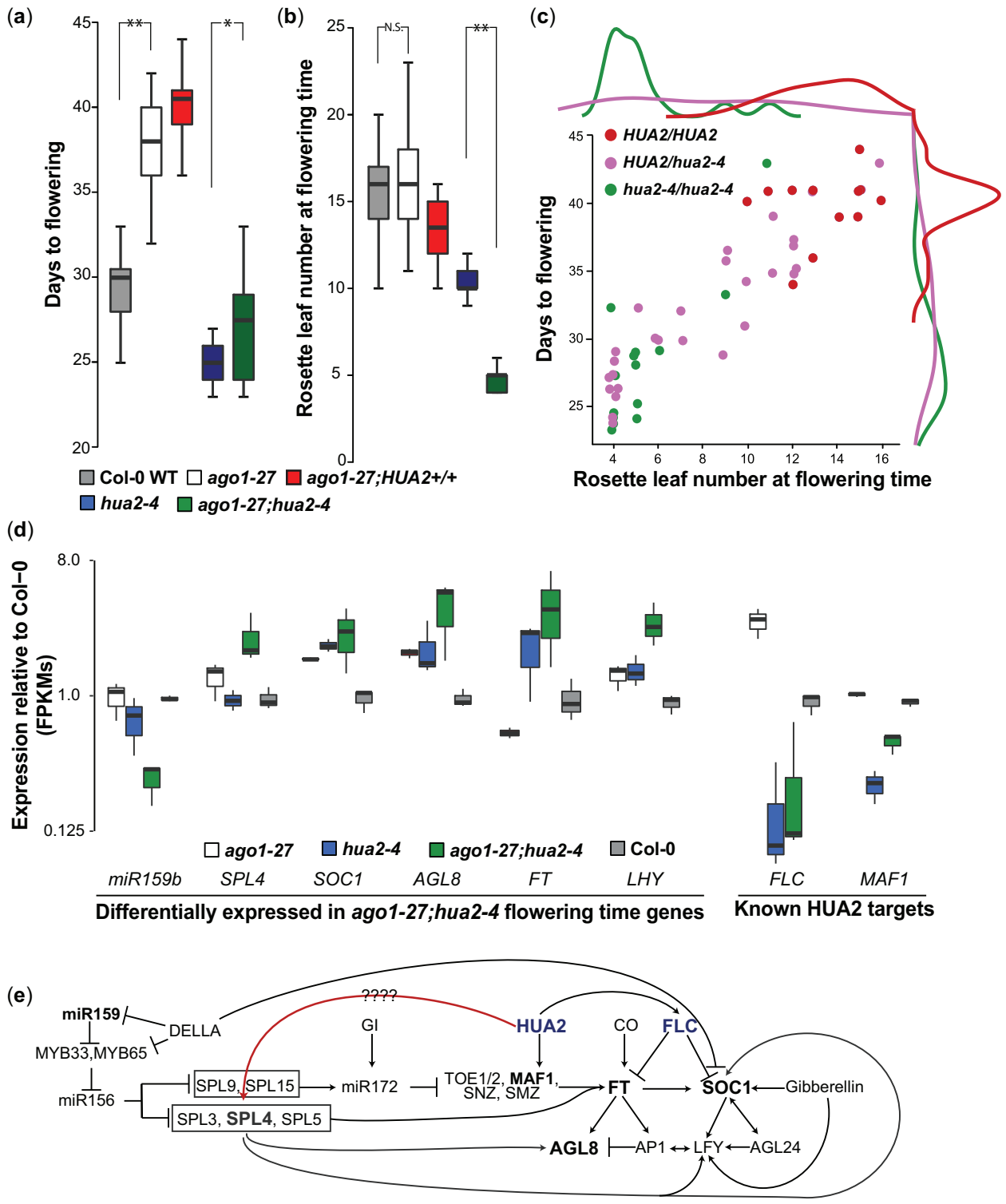

Fig. 5. The *ago1-27*; *hua2-4* double mutant uncouples the traits days to flowering time and rosette leaf number in the Col-0 background. An F_2 population segregating for the *ago1-27* and *hua2-4* mutant alleles was grown in LD. Days to flowering were recorded and rosette leaf numbers at the onset of flowering were counted. Gray, Col-0 WT; white, *ago1-27* parent; red, *ago1-27; HUA2+/+* F2; blue, *hua2-4* parent; green, *ago1-27; hua2-4*. See Supplementary Table 5 for further details. a) Plants carrying a homozygous *ago1-27* allele flowered ~8.6 days later than Col-0 WT with ~16 leaves. Plants carrying a homozygous *hua2-4* allele initiated flowering ~4.5 days earlier than Col-0 WT. As observed for STAIRS9472; *ago1-27*, the *hua2-4* mutant allele was epistatic to *ago1-27*. *$P < 0.0283$, **$P < 1.0E{-}06$, Mann–Whitney Wilcoxon test. The double mutant *ago1-27; hua2-4* plants showed a similar mean value but greater trait variance. b) The rosette leaf number phenotype of the double mutant *ago1-27; hua2-4* plants resembles that of the STAIRS9472; *ago1-27* line. *ago1-27; hua2-4* plants flower with 5 leaves on average (*$P < 0.0283$, **$P < 1.0E{-}06$, Mann–Whitney Wilcoxon test, for (a) and (b)]. c) Scatter plot with rosette leaf number on the x-axis and days to flowering on the y-axis. Data are shown for F_2 plants that are homozygous for the *ago1-27* mutant allele and segregate for the *hua2-4* mutant allele. d) Known flowering time genes with differential expression in the *ago1-27; hua2-4* double mutant as determined by RNA-seq. e) Suggested intersection of miRNAs and HUA2 in flowering time pathways. Depicted in red is the proposed connection between *HUA2* and *SPL4* such that *SPL4* expression is regulated by both mir156 and HUA2. In bold, genes that are overexpressed in the double mutant *ago1-27, hua-2* relative to the single mutant *ago1-27*.

the AGO1-dependent lesions (Mason *et al.* 2016), it raised anew the question as to how AGO1 may buffer genetic variation. In flies, proper expression of mir-9a, a miRNA acting on the transcription factor *Senseless*, buffers genomic variation (Cassidy *et al.* 2013). Reducing mir-9a regulation of *Senseless* leads to phenotypic variation in sensory cell fate in genetically diverse flies, with candidate causal variants in genes that belong to the *Senseless*-dependent proneural network governing sensory organ fate. In other words, in this case, AGO1-dependent buffering via mir-9a occurs at the network level, consistent with the mechanisms by which miRNAs buffer development stability and micro-environmental fluctuations.

To fully understand an instance of AGO1-dependent genetic variation, we focused on the uncoupling of the traits days to flowering and rosette leaf number in STAIRS9472. Both traits involve the mir156-SPL module and the key players *FLC* and *FRI* (Fig. 5d). We show that in the Col-0 background the coupling of these traits requires functional *FLC* and *AGO1*. In STAIRS9472, *FLC* is nonfunctional because the gene resides in the *Ler*-introgression segment. Without *FLC*, how are days to flowering and rosette leaf number coupled in *Ler*? Using bulk segregant analysis, we identified the nonfunctional *hua2 Ler*-allele as the likely causal AGO1-dependent polymorphism. Indeed, we were able to recapitulate the uncoupling phenotype in the *hua2-4; ago1-27* double mutant in the Col-0 background.

It is noteworthy that this nonfunctional *HUA2* allele arose only recently and likely in the laboratory (Zapata *et al.* 2016); there are several *Ler* strains without this allele (Chen and Meyerowitz 1999; Doyle *et al.* 2005; Zapata *et al.* 2016). These strains and other *Arabidopsis* accessions with nonfunctional *FLC* genes must have acquired different polymorphisms to maintain the coupling of both traits. The inbreeding nature of *Arabidopsis* and the propagation of commonly used accessions like *Ler* in controlled laboratory conditions readily allows fixation of such polymorphisms. However, there are prior reports that natural variation in *HUA2* can affect flowering time and plant morphology. The Sy-0 accession carries a gain-of function *HUA2* allele that enhances *FLC* expression leading to larger rosettes, in addition to suppressing *AGAMOUS* leading to indeterminate development of floral meristems (Wang *et al.* 2007). The Ws accession carries a 12-bp deletion in *HUA2*, possibly weakening *HUA2* function (Doyle *et al.* 2005).

Our expression analysis offered some clues as to how *HUA2* may facilitate the close coupling of days to flowering and rosette leaf number (Fig. 5, d and e). Comparing gene expression in *ago1-27* and *ago1-27; hua2-4* plants, we found that the mir156-SPL module gene *SPL4* was highly upregulated in the double mutant. *SPL4* is expressed in 3 splice isoforms (*SPL4-1*, *SPL4-2*, *SPL4-3*) with only 1, *SPL4-1*, regulated by miR156 (Yang *et al.* 2012). Overexpression of *SPL4-1* in transgenic plants does not alter days to flowering but reduces rosette leaf number. In contrast, overexpression of *SLP4-2* or *SPL4-3* decreases both days to flowering and reduces rosette leaf number (Yang *et al.* 2012). Because *HUA2* functions in mRNA processing and splicing (Chen and Meyerowitz 1999; Cheng *et al.* 2003; Janakirama 2013), *SPL4* may be one of its targets. Nonfunctional *HUA2* may lead to increased presence of the *SPL4-1* splice form, which is exacerbated when mir156-dependent suppression of *SPL4-1* fails in the *ago1-27; hua2-4* double mutant, disrupting the close correlation of days to flowering and rosette leaf number (Fig. 5e). Thus, similar to the scenario in flies (Cassidy *et al.* 2013), AGO1 appears to buffer genetic variation via miRNA-dependent network connections in plants. Disruption of the miRNA-dependent network path in *ago1*-mutants can reveal genetic variants such as the nonfunctional *HUA2* allele in other paths controlling the same trait (Fig. 5e).

Taken together, our study holds several important lessons. First, AGO1 buffers phenotypic variation in isogenic seedlings and genetic variation in genetically divergent ones. Second, AGO1 does so independently of the chaperone HSP90 despite their close functional relationship, suggesting that epistasis is largely a first-order phenomenon, specific to 2 interacting loci. Indeed, this observed specificity of epistasis can extend to specific variants in pairwise interacting loci. We previously showed that HSP90 can buffer genetic variation in Ste12, a transcription factor that governs mating and invasion in yeast. However, HSP90-dependent variants in Ste12 are rare; they reside in only 2 positions that are close to one another and alter charge and DNA binding (Dorrity *et al.* 2018). This surprising specificity of epistatic interactions calls into question the utility of current large-scale efforts to understand the phenotypic contributions of epistasis by combining null mutants in human cells and in other organisms. Third, our results provide a cautionary tale in interpreting phenocopies. Mutants in AGO1 and HSP90 show highly similar phenotypes (Bohmert *et al.* 1998; Queitsch *et al.* 2002; Morel 2002; Vaucheret *et al.* 2004; Sangster *et al.* 2007; Mason *et al.* 2016), and yet the underlying mechanisms appear to differ, at least in part. Fourth, unlike HSP90, AGO1 suppresses the phenotypic consequences of genetic variation by enabling miRNA-dependent network paths rather than acting directly on variant-containing molecules, thereby extending the buffering concept. Fifth and last, we show that key pathways can involve different molecular players even in closely related strains of the same species. The uncoupling of highly correlated traits could be a useful tool for plant breeders who want to improve 1 trait without compromising another tightly coupled trait. Our study suggests miRNAs as good candidates for such targeted breeding and engineering efforts.

Data availability

All RNA sequencing reads and genomic sequence used for the SHOREmap analysis are deposited in the NCBI Sequence Read Archive under the BioProject accession PRJNA836875.

Supplemental material is available at GENETICS online.

Acknowledgments

We thank the editor and 2 anonymous reviewers for insightful comments and additional references that have improved this article.

Funding

This work was supported by the National Human Genome Research Institute Interdisciplinary Training in Genomic Sciences (T32 training grant HG000035 to GAM), the National Institute of Health (New Innovator award DP2OD008371 and NIGMS 1R35GM139532-01 to CQ) and the National Science Foundation (RESEARCH-PGR grant 17488843 to CQ).

Conflicts of interest

None declared.

Literature cited

Anders S, Pyl PT, Huber W. HTSeq—a Python framework to work with high-throughput sequencing data. Bioinformatics. 2015; 31(2):166–169.

Andrés F, Coupland G. The genetic basis of flowering responses to seasonal cues. Nat Rev Genet. 2012;13(9):627–639.

Aukerman MJ, Sakai H. Regulation of flowering time and floral organ identity by a MicroRNA and its APETALA2-like target genes. Plant Cell. 2003;15(11):2730–2741.

Axtell MJ. Classification and comparison of small RNAs from plants. Annu Rev Plant Biol. 2013;64:137–159.

Bloomer RH, Dean C. Fine-tuning timing: natural variation informs the mechanistic basis of the switch to flowering in *Arabidopsis thaliana*. J Exp Bot. 2017;68(20):5439–5452.

Bohmert K, Camus I, Bellini C, Bouchez D, Caboche M, Benning C. AGO1 defines a novel locus of *Arabidopsis* controlling leaf development. . 1998;17(1):170–180.

Bologna NG, Voinnet O. The diversity, biogenesis, and activities of endogenous silencing small RNAs in *Arabidopsis*. Annu Rev Plant Biol. 2014;65:473–503.

Borevitz JO, Hazen SP, Michael TP, Morris GP, Baxter IR, Hu TT, Chen H, Werner JD, Nordborg M, Salt DE, *et al.* Genome-wide patterns of single-feature polymorphism in *Arabidopsis thaliana*. Proc Natl Acad Sci U S A. 2007;104(29):12057–12062.

Cassidy JJ, Jha AR, Posadas DM, Giri R, Venken KJT, Ji J, Jiang H, Bellen HJ, White KP, Carthew RW, *et al.* miR-9a minimizes the phenotypic impact of genomic diversity by buffering a transcription factor. Cell. 2013;155(7):1556–1567.

Chen X, Meyerowitz EM. HUA1 and HUA2 are two members of the floral homeotic AGAMOUS pathway. Mol Cell. 1999;3(3):349–360.

Cheng Y, Kato N, Wang W, Li J, Chen X. Two RNA binding proteins, HEN4 and HUA1, act in the processing of AGAMOUS pre-mRNA in Arabidopsis thaliana. Dev Cell. 2003;4(1):53–66.

Cuperus JT, Montgomery TA, Fahlgren N, Burke RT, Townsend T, Sullivan CM, Carrington JC. Identification of MIR390a precursor processing-defective mutants in *Arabidopsis* by direct genome sequencing. Proc Natl Acad Sci U S A. 2010;107(1):466–471.

Cuperus JT, Fahlgren N, Carrington JC. Evolution and functional diversification of MIRNA genes. Plant Cell 2011;23(2):431–442.

Dong Q, Hu B, Zhang C. MicroRNAs and their roles in plant development. Front Plant Sci. 2022;13:824240.

Dorrity MW, Cuperus JT, Carlisle JA, Fields S, Queitsch C. Preferences in a trait decision determined by transcription factor variants. Proc Natl Acad Sci U S A. 2018;115:E7997–E8006.

Doyle MR, Bizzell CM, Keller MR, Michaels SD, Song J, Noh Y-S, Amasino RM. HUA2 is required for the expression of floral repressors in *Arabidopsis thaliana*. Plant J. 2005;41(3):376–385.

Gangaraju VK, Yin H, Weiner MM, Wang J, Huang XA, Lin H. *Drosophila* Piwi functions in Hsp90-mediated suppression of phenotypic variation. Nat Genet. 2011;43(2):153–158.

Gómez-Mena C, Piñeiro M, Franco-Zorrilla JM, Salinas J, Coupland G, Martínez-Zapater JM. Early bolting in short days: an *Arabidopsis* mutation that causes early flowering and partially suppresses the floral phenotype of leafy. Plant Cell. 2001;13(5):1011–1024.

Hilgers V, Bushati N, Cohen SM. Drosophila microRNAs 263a/b confer robustness during development by protecting nascent sense organs from apoptosis. PLoS Biol. 2010;8(6):e1000396.

Hornstein E, Shomron N. Canalization of development by microRNAs. Nat Genet. 2006;38:S20–4.

Iki T, Yoshikawa M, Nishikiori M, Jaudal MC, Matsumoto-Yokoyama E, Mitsuhara I, Meshi T, Ishikawa M. In vitro assembly of plant RNA-induced silencing complexes facilitated by molecular chaperone HSP90. Mol Cell. 2010;39(2):282–291.

Iki T, Yoshikawa M, Meshi T, Ishikawa M. Cyclophilin 40 facilitates HSP90-mediated RISC assembly in plants. EMBO J. 2012;31(2):267–278.

Iwasaki S, Kobayashi M, Yoda M, Sakaguchi Y, Katsuma S, Suzuki T, Tomari Y. Hsc70/Hsp90 chaperone machinery mediates ATP-dependent RISC loading of small RNA duplexes. Mol Cell. 2010;39(2):292–299.

Iwasaki S, Sasaki HM, Sakaguchi Y, Suzuki T, Tadakuma H, Tomari Y. Defining fundamental steps in the assembly of the *Drosophila* RNAi enzyme complex. Nature. 2015;521(7553):533–536.

Janakirama P. Functional characterization of the HUA2 gene family in *Arabidopsis thaliana* [thesis]; Supervisor: Dr. Vojislava Grbic, The University of Western Ontario, 2013.

Jarosz DF, Taipale M, Lindquist S. Protein homeostasis and the phenotypic manifestation of genetic diversity: principles and mechanisms. Annu Rev Genet. 2010;44:189–216.

Jarosz DF, Lindquist S. Hsp90 and environmental stress transform the adaptive value of natural genetic variation. Science. 2010;330(6012):1820–1824.

Ji L, Liu X, Yan J, Wang W, Yumul RE, Kim YJ, Dinh TT, Liu J, Cui X, Zheng B, *et al.* 2011. ARGONAUTE10 and ARGONAUTE1 regulate the termination of floral stem cells through two MicroRNAs in *Arabidopsis*, PLoS Genet. 7:e1001358.

Johnston M, Geoffroy M-C, Sobala A, Hay R, Hutvagner G. HSP90 protein stabilizes unloaded Argonaute complexes and microscopic P-bodies in human cells. Mol Biol Cell. 2010;21(9):1462–1469.

Karras GI, Yi S, Sahni N, Fischer M, Xie J, Vidal M, D'Andrea AD, Whitesell L, Lindquist S. HSP90 shapes the consequences of human genetic variation. Cell. 2017;168(5):856–866.e12.

Kim D-H, Doyle MR, Sung S, Amasino RM. Vernalization: winter and the timing of flowering in plants. Annu Rev Cell Dev Biol. 2009;25:277–299.

Koumproglou R, Wilkes TM, Townson P, Wang XY, Beynon J, Pooni HS, Newbury HJ, Kearsey MJ. STAIRS: a new genetic resource for functional genomic studies of *Arabidopsis*. Plant J. 2002;31(3):355–364.

Lachowiec J, Lemus T, Borenstein E, Queitsch C. Hsp90 promotes kinase evolution. Mol Biol Evol. 2015;32(1):91–99.

Lachowiec J, Mason GA, Schultz K, Queitsch C. Redundancy, feedback, and robustness in the *Arabidopsis thaliana* BZR/BEH gene family. Front Genet. 2018;9:523.

Lempe J, Balasubramanian S, Sureshkumar S, Singh A, Schmid M, Weigel D. Diversity of flowering responses in wild *Arabidopsis thaliana* strains. PLoS Genet. 2005;1(1):109–118.

Lempe J, Lachowiec J, Sullivan AM, Queitsch C. Molecular mechanisms of robustness in plants. Curr Opin Plant Biol. 2013;16(1):62–69.

Li X, Cassidy JJ, Reinke CA, Fischboeck S, Carthew RW. A MicroRNA imparts robustness against environmental fluctuation during development. Cell. 2009;137(2):273–282.

Liu J, He Y, Amasino R, Chen X. siRNAs targeting an intronic transposon in the regulation of natural flowering behavior in *Arabidopsis*. Genes Dev. 2004;18(23):2873–2878.

Love MI, Huber W, Anders S. Moderated estimation of fold change and dispersion for RNA-seq data with DESeq2. Genome Biol. 2014;15(12):550.

Luo Y, Guo Z, Li L. Evolutionary conservation of microRNA regulatory programs in plant flower development. Dev Biol. 2013;380(2):133–144.

Masel J, Siegal ML. Robustness: mechanisms and consequences. Trends Genet. 2009;25(9):395–403.

Mason GA, Lemus T, Queitsch C. The mechanistic underpinnings of an ago1-mediated, environmentally dependent, and stochastic phenotype. Plant Physiol. 2016;170(4):2420–2431.

Michaels SD, He Y, Scortecci KC, Amasino RM. Attenuation of FLOWERING LOCUS C activity as a mechanism for the evolution

of summer-annual flowering behavior in Arabidopsis. Proc Natl Acad Sci U S A. 2003;100(17):10102–10107.
Miyoshi T, Takeuchi A, Siomi H, Siomi MC. A direct role for Hsp90 in pre-RISC formation in *Drosophila*. Nat Struct Mol Biol. 2010;17(8):1024–1026.
Morel J-B, Godon C, Mourrain P, Béclin C, Boutet S, Feuerbach F, Proux F, Vaucheret H. Fertile hypomorphic ARGONAUTE (ago1) mutants impaired in post-transcriptional gene silencing and virus resistance. Plant Cell. 2002;14(3):629–639.
Naruse K, Matsuura-Suzuki E, Watanabe M, Iwasaki S, Tomari Y. In vitro reconstitution of chaperone-mediated human RISC assembly. RNA. 2018;24(1):6–11.
Nordborg M, Hu TT, Ishino Y, Jhaveri J, Toomajian C, Zheng H, Bakker E, Calabrese P, Gladstone J, Goyal R, *et al.* The pattern of polymorphism in *Arabidopsis thaliana*. PLoS Biol. 2005;3(7):e196.
Okazaki K, Kato H, Iida T, Shinmyozu K, Nakayama J-I, *et al.* RNAi-dependent heterochromatin assembly in fission yeast *Schizosaccharomyces pombe* requires heat-shock molecular chaperones Hsp90 and Mas5. Epigenetics Chromatin. 2018;11. Article number: 26. https://doi.org/10.1186/s13072-018–0199-8
Ossowski S, Schneeberger K, Clark RM, Lanz C, Warthmann N, Weigel D. Sequencing of natural strains of *Arabidopsis thaliana* with short reads. Genome Res. 2008;18(12):2024–2033.
Pouteau S, Ferret V, Gaudin V, Lefebvre D, Sabar M, Zhao G, Prunus F. Extensive phenotypic variation in early flowering mutants of *Arabidopsis*. Plant Physiol. 2004;135(1):201–211.
Queitsch C, Sangster TA, Lindquist S. Hsp90 as a capacitor of phenotypic variation. Nature. 2002;417(6889):618–624.
Rival P, Press MO, Bale J, Grancharova T, Undurraga SF, Queitsch C. The conserved PFT1 tandem repeat is crucial for proper flowering in *Arabidopsis thaliana*. Genetics. 2014;198(2):747–754.
Rohner N, Jarosz DF, Kowalko JE, Yoshizawa M, Jeffery WR, Borowsky RL, Lindquist S, Tabin CJ. Cryptic variation in morphological evolution: HSP90 as a capacitor for loss of eyes in cavefish. Science. 2013;342(6164):1372–1375.
Rutherford SL, Lindquist S. Hsp90 as a capacitor for morphological evolution. Nature. 1998;396(6709):336–342.
Salathia N, Lee HN, Sangster TA, Morneau K, Landry CR, Schellenberg K, Behere AS, Gunderson KL, Cavalieri D, Jander G, *et al.* Indel arrays: an affordable alternative for genotyping. Plant J. 2007;51(4):727–737.
Sangster TA, Lindquist S, Queitsch C. Under cover: causes, effects and implications of Hsp90-mediated genetic capacitance. Bioessays. 2004;26(4):348–362.
Sangster TA, Bahrami A, Wilczek A, Watanabe E, Schellenberg K, McLellan C, Kelley A, Kong SW, Queitsch C, Lindquist S, *et al.* Phenotypic diversity and altered environmental plasticity in Arabidopsis thaliana with reduced Hsp90 levels. PLoS One. 2007;2(7):e648.
Sangster TA, Salathia N, Lee HN, Watanabe E, Schellenberg K, Morneau K, Wang H, Undurraga S, Queitsch C, Lindquist S, *et al.* HSP90-buffered genetic variation is common in *Arabidopsis thaliana*. Proc Natl Acad Sci U S A. 2008;105(8):2969–2974.
Sangster TA, Salathia N, Undurraga S, Milo R, Schellenberg K, Lindquist S, Queitsch C. HSP90 affects the expression of genetic variation and developmental stability in quantitative traits. Proc Natl Acad Sci U S A. 2008;105(8):2963–2968.
Schneeberger K, Ossowski S, Lanz C, Juul T, Petersen AH, Nielsen KL, Jørgensen J-E, Weigel D, Andersen SU. SHOREmap: simultaneous mapping and mutation identification by deep sequencing. Nat Methods. 2009;6(8):550–551.
Schopf FH, Biebl MM, Buchner J. The HSP90 chaperone machinery. Nat Rev Mol Cell Biol. 2017;18(6):345–360.
Shindo C, Aranzana MJ, Lister C, Baxter C, Nicholls C, Nordborg M, Dean C. Role of FRIGIDA and FLOWERING LOCUS C in determining variation in flowering time of *Arabidopsis*. Plant Physiol. 2005;138(2):1163–1173.
Smith MR, Willmann MR, Wu G, Berardini TZ, Möller B, Weijers D, Poethig RS. Cyclophilin 40 is required for microRNA activity in *Arabidopsis*. Proc Natl Acad Sci U S A. 2009;106(13):5424–5429.
Song YH, Ito S, Imaizumi T. Flowering time regulation: photoperiod- and temperature-sensing in leaves. Trends Plant Sci. 2013;18(10):575–583.
Song YH, Shim JS, Kinmonth-Schultz HA, Imaizumi T. Photoperiodic flowering: time measurement mechanisms in leaves. Annu Rev Plant Biol. 2015;66:441–464.
Soppe WJ, Bentsink L, Koornneef M. The early-flowering mutant efs is involved in the autonomous promotion pathway of *Arabidopsis thaliana*. Development. 1999;126(21):4763–4770.
Spanudakis E, Jackson S. The role of microRNAs in the control of flowering time. J Exp Bot. 2014;65(2):365–380.
Sun H, Schneeberger K. SHOREmap v3.0: fast and accurate identification of causal mutations from forward genetic screens. Methods Mol Biol. 2015;1284:381–395.
Sung S, Schmitz RJ, Amasino RM. A PHD finger protein involved in both the vernalization and photoperiod pathways in Arabidopsis. Genes Dev. 2006;20(23):3244–3248.
Takahashi M, Morikawa H. Nitrogen dioxide accelerates flowering without changing the number of leaves at flowering in *Arabidopsis thaliana*. Plant Signal Behav. 2014;9(10):e970433.
Trapnell C, Pachter L, Salzberg SL. TopHat: discovering splice junctions with RNA-Seq. Bioinformatics. 2009;25(9):1105–1111.
Trapnell C, Hendrickson DG, Sauvageau M, Goff L, Rinn JL, Pachter L. Differential analysis of gene regulation at transcript resolution with RNA-seq. Nat Biotechnol. 2013;31(1):46–53.
Undurraga SF, Press MO, Legendre M, Bujdoso N, Bale J, Wang H, Davis SJ, Verstrepen KJ, Queitsch C. Background-dependent effects of polyglutamine variation in the *Arabidopsis thaliana* gene ELF3. Proc Natl Acad Sci U S A. 2012;109(47):19363–19367.
Untergasser A, Cutcutache I, Koressaar T, Ye J, Faircloth BC, Remm M, Rozen SG. Primer3-new capabilities and interfaces. Nucleic Acids Res. 2012;40(15):e115.
Vaucheret H, Vazquez F, Crété P, Bartel DP. The action of ARGONAUTE1 in the miRNA pathway and its regulation by the miRNA pathway are crucial for plant development. Genes Dev. 2004;18(10):1187–1197.
Voinnet O. Origin, biogenesis, and activity of plant microRNAs. Cell. 2009;136(4):669–687.
Wang Q, Sajja U, Rosloski S, Humphrey T, Kim MC, Bomblies K, Weigel D, Grbic V. HUA2 caused natural variation in shoot morphology of *A. thaliana*. Curr Biol. 2007;17(17):1513–1519.
Wang Y, Mercier R, Hobman TC, LaPointe P. Regulation of RNA interference by Hsp90 is an evolutionarily conserved process. Biochim. Biophys. Acta. 2013;1833(12):2673–2681.
Weigel D, Glazebrook J. Arabidopsis: A Laboratory Manual. Cold Spring Harbor (New York): Cold Spring Harbor Laboratory Press; 2002.
Whitacre JM. Biological robustness: paradigms, mechanisms, and systems principles. Front Genet. 2012;3:67.
Whittaker C, Dean C. The FLC locus: a platform for discoveries in epigenetics and adaptation. Annu Rev Cell Dev Biol. 2017;33:555–575.
Woehrer SL, Aronica L, Suhren JH, Busch CJ-L, Noto T, Mochizuki K. A Tetrahymena Hsp90 co-chaperone promotes siRNA loading by

ATP-dependent and ATP-independent mechanisms. 2015;34(4): 559–577.

Wu G, Park MY, Conway SR, Wang J-W, Weigel D, Poethig RS. The sequential action of miR156 and miR172 regulates developmental timing in *Arabidopsis*. Cell. 2009;138(4):750–759.

Xu M, Hu T, Zhao J, Park M-Y, Earley KW, *et al.* 2016. Developmental functions of miR156-regulated SQUAMOSA PROMOTER BINDING PROTEIN-LIKE (SPL) genes in *Arabidopsis thaliana*. PLoS Genet. 12: e1006263.

Yamaguchi A, Wu M-F, Yang L, Wu G, Poethig RS, Wagner D. The microRNA-regulated SBP-Box transcription factor SPL3 is a direct upstream activator of LEAFY, FRUITFULL, and APETALA1. Dev Cell. 2009;17(2):268–278.

Yang X, Zhang H, Li L. Alternative mRNA processing increases the complexity of microRNA-based gene regulation in *Arabidopsis*. Plant J. 2012;70(3):421–431.

Yeyati PL, Bancewicz RM, Maule J, van Heyningen V. Hsp90 selectively modulates phenotype in vertebrate development. PLoS Genet. 2007;3(3):e43.

Zabinsky RA, Mason GA, Queitsch C, Jarosz DF. It's not magic—Hsp90 and its effects on genetic and epigenetic variation. Semin Cell Dev Biol. 2019;88:21–35.

Zapata L, Ding J, Willing E-M, Hartwig B, Bezdan D, *et al.* Chromosome-level assembly of *Arabidopsis thaliana* L *er* reveals the extent of translocation and inversion polymorphisms. Proc Natl Acad Sci U S A. 2016;113:E4052–E4060.

Communicating editor: K. Bomblies